Regular Article

PHYSICAL CHEMISTRY RESEARCH
Published by the
Iranian Chemical Society
www.physchemres.org
info@physchemres.org

Phys. Chem. Res., Vol. 8, No. 4, 609-627, December 2020
DOI: 10.22036/pcr.2020.210913.1705

Ultrafast Luminescence Decay in Rhenium(I) Complexes with Imidazo[4,5-f]-1,10-Phenanthroline Ligands: TDDFT Method

Z. Yazdanpanahfard*, M. Oftadeh* and S. Fakhraee

Chemistry Department, Payame Noor University, 19395-4697 Tehran, I. R. Iran

(Received 8 December 2019, Accepted 22 June 2020)

The interpretation of the ultrafast luminescence decay in [Re(Br(CO)$_3$(N^N)] complexes as a new group of chromophoric imidazo[4,5-f]-1,10-phenanthroline ligands, including 1,2-dimethoxy benzene, tert-butyl benzene (L4) and 1,2,3-trimethoxy benzene, tert-butyl benzene (L6), was studied. Fac-[Re(Br(CO)$_3$L4 and L6] with different aryl groups were calculated in the singlet and triplet excited states. The calculations were performed in the gas phase and in the presence of chloroform as a solvent. The absorption and luminescence wavelengths, transition energy, and oscillator strength for singlet and triplet states were calculated for the entitled complexes with L4 and L6 ligands. The UV-Vis spectrum and the singlet and triplet energy diagrams show a good agreement between our computational results and the experimental results, particularly in the case of the triplet state in chloroform. The spin-orbit coupling calculations show sufficient intensity and short wavelength in the UV-Vis absorption after SOC correction. The results of NBO calculations in the solvent show that rhenium acts as an acceptor by means of E(2), the second-order interaction energies between donor and acceptor orbitals, at the B3LYP/lanl2mb level of theory.

Keywords: TD-DFT method, Excited states, Intersystem crossing, Spin-orbit coupling, Rhenium(I) complexes

INTTRODUCTION

Rhenium(I) carbonyl diimine complexes show extremely rich excited-state action that can be adjusted via structural change and the media [1-3]. They can be agglutinated into a range of environments, including multimolecular and polymers, or joined to biomolecules like proteins or DNA. Potent photoluminescence and long-lasting excited states with great reduction and oxidation potentials, along with artificial flexibility and stability, make rhenium tricarbonyl diimine very suitable sensitizers [2,3] of energy transition and electron-transition (ET) processes. Moreover, they are well matched for the photocatalysis of reducing CO_2 [4-6] as phosphorescent labels and probes of biomolecules [7-10], sensors [11,12], or hopeful molecular exchange [13-16] and organic light-emitting collection emitters [17]. Excited rhenium complexes have been utilized as IR probes of picosecond dynamics for dipolar solvents, ionic liquids, supramolecules, and proteins [18-22]. Their capability for triggering ultrafast ET has been proved using a recent outcome corresponding to a remarkable acceleration of long-range ET in Re-labeled azurin [23,24]. Few studies have been dedicated to intersystem crossing (ISC) processes in complexes of transition metal. The first detailed research of the dynamics of singlet to triplet transitions have been made for understanding the photochemical reactivity of $HCo(CO)_4$ [25] and $HM(CO)_3$(α-diimine) (M = Mn, Re) molecules [26-28] that undergo concurrent primary photoreactions whose branching ratio is controlled by ISC from the absorbing state to the reactive states. More recently, review articles on possible outcomes of spin-orbit coupling (SOC) on the electronic structure, excited state characters, and their deactivation pathways have been propounded. They indicate the connection between SOC

*Corresponding authors. E-mail: yazdanpanahfard@es.isfpnu.ac.ir; m_oftadeh@pnu.ac.ir

and metal-to-ligand charge-transfer character of the lowest "triplet" states of superior emphasis for organic light-emitting diode (OLED) applications from its zero-field separation and photoluminescence point of view [29-35]. The photophysics corresponding to rhenium tricarbonyl complexes $Re(X)(CO)_3$(a-diimine) (X = Chloride, bromide, iodide) has been recently studied using ultrafast luminescence spectroscopy [36], and it is still many unresolved issues related to SOC. Indeed, the lowest allowed optical excitations of $Re(X)(CO)_3$ to diimine charge-transfer (CT) transition contain two or three ultrafast steps, where the fastest one is ascribed to the singlet to triplet ($^1CT \rightarrow {}^3CT$) intersystem crossing (ISC). Lophine (2,4,5-triphenyl imidazole) [37] (Scheme 1) was recognized more than 50 years ago [38] and primarily examined for its fluorescence and chemiluminescence properties [39]. Syntheses have been progressed [40] and the emission specifications adjusted over the imidazole substituents [41]. The lophine derivatives have shown a great application in analytical disciplines [42]. The variety and facility of functionalization of the lophine core have permitted a wide range of novel systems to be introduced including those having applications in coordination chemistry. The closely associated fused unit imidazo[4,5-f]-1,10-phenanthroline (Scheme 1) has become a widely used ligand in recent years [43]. In Re(I) case, only few studies have been performed on the coordination chemistry of imidazo[4,5-f]-1,10-phenanthroline type ligands, including heterobimetallic assemblies [44]. Bonello has demonstrated that the imidazo[4,5-f]-1,10-phenanthroline ligand is perfectly matched with Re(I) leading to production of $[ReBr(CO)_3$ L1-L8] complexes [45]. New synthesized series of chromophore-based ligands have been found on the fused imidazo[4,5-f]-1,10-phenanthroline nucleus functionalized with various aryl groups [45]. The production and spectroscopic characterization of eight new fac-$[Re(Br(CO)_3(N^N)]$ complexes have been documented, including the X-ray structures of L4 and L6 ligands. The L1-L8 ligands studied by Bonello *et al.* are shown in Scheme 2. So far, limited reports have been published about imidazo[4,5-f]-1,10-phenanthroline, and especially on heavy metal compounds with heavy elements such as rhenium. In this work, using computational chemistry, we tried to show the transition of the lowest triplet excited state and on a singlet bases state corresponding to the selected rhenium complexes including Fac-$[Re(Br(CO)_3$ L4 and L6], 1,2-dimethoxy benzene, tert-butyl benzene (L4) and 1,2,3-trimethoxy benzene, tert-butyl benzene (L6), two ligands from eight ligands. Bromide as a halogen, imidazo[4,5-f]-1,10-phenanthroline, and three carbonyl groups in these complexes were used to investigate their effects on the ultrafast luminescence decay phenomena. The main methodologies of this work are as follows: At first, calculating and comparing the maximum wavelengths, transition energies, and oscillator strengths of singlet and triplet states of the rhenium complexes with L4 and L6 ligands in gas and solution phases, and then, comparing the maximum wavelengths of triplet states between free L4 and L6 ligands and rhenium in combination with L4 and L6 ligands in the solution phase.

METHOD

Bonello experimental studies encouraged us to study the UV-Vis and luminescence features using the computational method for fac-$[Re(Br(CO)_3$ L4 and L6**]**. The S_0 electronic ground state, the lowest S_1, S_2, S_3 and S_4 singlet excited states were calculated. The vertical excitations at the ground state geometry and the T_1, T_2, T_3 and T_4 triplet excited states were optimized under the Cs symmetry constraint, at the density functional level of theory (DFT), within the time-dependent approach (TD-DFT) for the excited states, using the functional B3LYP with all electrons and lanl2mb basis set. Afterward, TD-DFT convergence was obtained and the triplet excited energies were computed. All computations were done using Gaussian 09 [46]. Moreover, Chemissian 4.23 software [47] was applied to plot the spectrums and energy diagrams of the molecular orbitals. In all calculations, the charge is zero and the spin multiplicity equals to one.

Using natural bond orbital (NBO) calculations, the interaction energies (E(2), kcal mol^{-1}) and the partial electron transfer (q) between the rhenium metal, bromide and ligand were determined at the B3LYP/lanl2mb level of theory. The ORCA software, version 4.1.2 [48,49], was applied to SOC in DKH as a relativistic Hamiltonian, and def2-TZVP SARC/J basis set was used for SOC calculations with all electrons for singlet and triplet of the

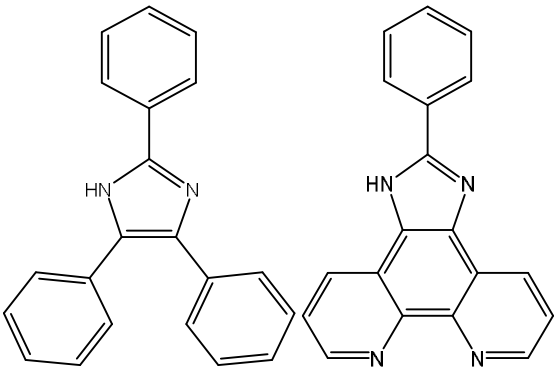

Scheme 1. Molecular structures of 2,4,5-triphenylimidazole (left) and 2-phenylimidazo[4,5-f]-1,10-phenanthroline (right) [45]

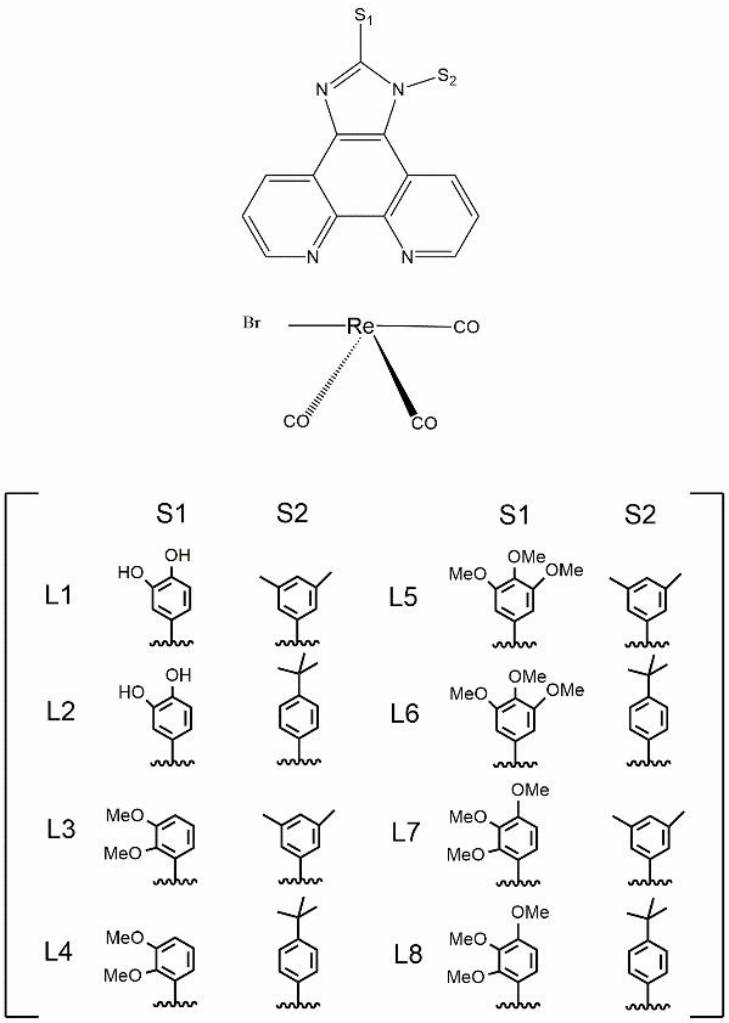

Scheme 2. Complexes of fac-[Re(Br(CO)$_3$(N^N)] and the ligands of L1-L8

complexes 1 and 2 in the gas and the solution phases.

RESULTS AND DISCUSSION

Gas Phase

Optimized structures of singlet and triplet of fac-[$ReBr(CO)_3$(L4)], complex 1, and fac-$ReBr(CO)_3$(L6), complex 2, are displayed in Figs. 1 and 2, respectively. Some differences were observed in matrix structures in terms of their dihedral angles of Z-matrix. Once the structure changed from singlet to triplet, a very slight twist occurred on the dihedral angles (Tables 1 and 2).

All of the dihedral changes are associated with the carbonyl and bromide groups linked to rhenium metal. Table 3 shows the transition energies, absorption and luminescence wavelengths, and vibrational oscillator strengths for 8 triplet and singlet electronic transitions of the rhenium (1) complexes with L4 ligand.

For complex 1 in the gas phase, the maximum absorption wavelength and the transition energy for $S_0 \rightarrow S_1$ are 475.29 nm and 2.6086 (ev), respectively, while the maximum luminescence wavelength and the transition energy from $T_1 \rightarrow S_0$ are 663.94 nm and 1.8674 (ev), respectively. Oscillator strengths (f) values are measures of transition intensity. The $S_0 \rightarrow S_1$ has the lowest oscillation (f = 0.0013), implying that this transition is weakly allowed. In comparison, the $S_0 \rightarrow S_2$ transition with f = 0.0426 is more strongly allowed than $S_0 \rightarrow S_1$. Therefore, the minimum energy and the highest wavelength are related to $T_1 \rightarrow S_0$ transition. The UV-Vis absorption spectra for S_1, the luminescence spectra for T_1 and diagram energy for S_1 and T_1 of the complex 1 are shown in Figs. 3 and 4, respectively.

The subgroups relating to the complex of rhenium with imidazole (4,5,f)-1,10-phenanthroline and L4 ligands include two methoxy groups, butyl phenyls, and three carbonyl groups. Also, bromide causes the spectral lines to be moved to long wavelengths. According to Fig. 4, the electronic transitions are different for the singlet and triplet states, and the lowest unoccupied molecular orbital (LUMO) for the triplet states is more above levels than the singlet states.

Table 4 shows the transition energies of different triplet and singlet states, absorption and luminescence wavelengths, and vibrational oscillations corresponding to the rhenium (1) complex with the L6 ligand.

For the complex 2 in the gas phase, the maximum absorption wavelength and the transition energy from S_0 to S_1 state are 478.36 nm and 2.5919 (eV), respectively, while the maximum luminescence wavelength and the transition energy for $T_1 \rightarrow S_0$, are 668.17 nm and 1.8556 (ev), respectively. The $S_0 \rightarrow S_1$ has the minimum oscillator strength with f = 0.0012 and show that this transition is weakly allowed, while the $S_0 \rightarrow S_2$ transition (f = 0.0459) is more strongly allowed than $S_0 \rightarrow S_1$. So, $T_1 \rightarrow S_0$ transition has the maximum wavelength and the minimum energy. Comparing the outcomes in Tables 3 and 4 demonstrates that the maximum wavelengths related to the singlet and triplet excited states of the complex 2 at S_1 and T_1 states are larger than those of the complex 1. $S_0 \rightarrow S_1$ and $T_1 \rightarrow S_0$ transition energies of the complex 2 is smaller than those of the complex 1. Also, oscillator strength values in complex 2 are greater than those in complex 1 and the transition intensity of complex 2 is stronger than that of complex 1. The UV-Vis absorption spectra for S_1 and luminescence spectra for T_1, and diagram energy for S_1 and T_1 of the complex 2 are demonstrated in Figs. 5 and 6, respectively The UV-Vis spectrum in Fig. 5A depicts a band in wavelength of 447.83 nm and oscillator strength of f = 0.0459.

Comparison of UV-Vis spectra of Figs. 3 and 5 shows that the absorption wavelengths of $S_0 \rightarrow S_1$ and the luminescence wavelengths of $T_1 \rightarrow S_0$ of the complex 2 are more than those of the complex 1. This difference is related to three methoxy groups in complex 2 and two methoxy groups in complex 1 and their positions.

Solution Phase

In the next step, solvent was used and all calculations were repeated in chloroform as solvent. Tables 5 and 6 show the transition energy, the absorption and luminescence wavelengths, and the oscillator strength of the complexes 1 and 2 for the singlet and triplet states. As presented in Table 5, $S_0 \rightarrow S_1$ and $T_1 \rightarrow S_0$ transition energies are 3.0535 (eV) and 2.0617 (eV), respectively. The maximum wavelengths in the singlet and triplet transition from S_0 to S_1 and T_1 states are 406.05 nm and 601.36 nm, respectively. The maximum wavelengths in the solution phase are shorter

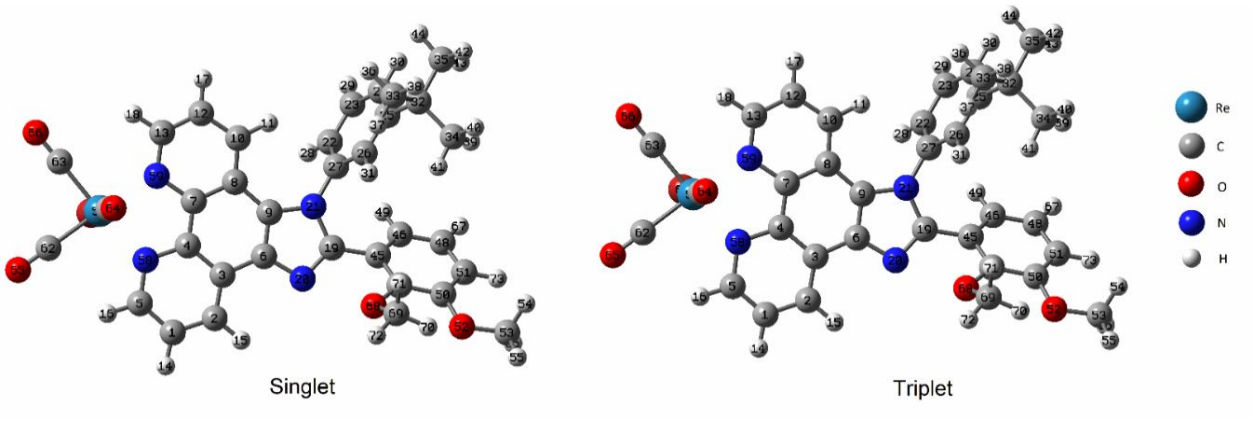

Fig. 1. Optimized structures of the singlet states (S_0, S_1, S_2, S_3, S_4) and triplet states (T_1, T_2, T_3 and T_4) of fac-[ReBr(CO)$_3$(L4)], complex 1.

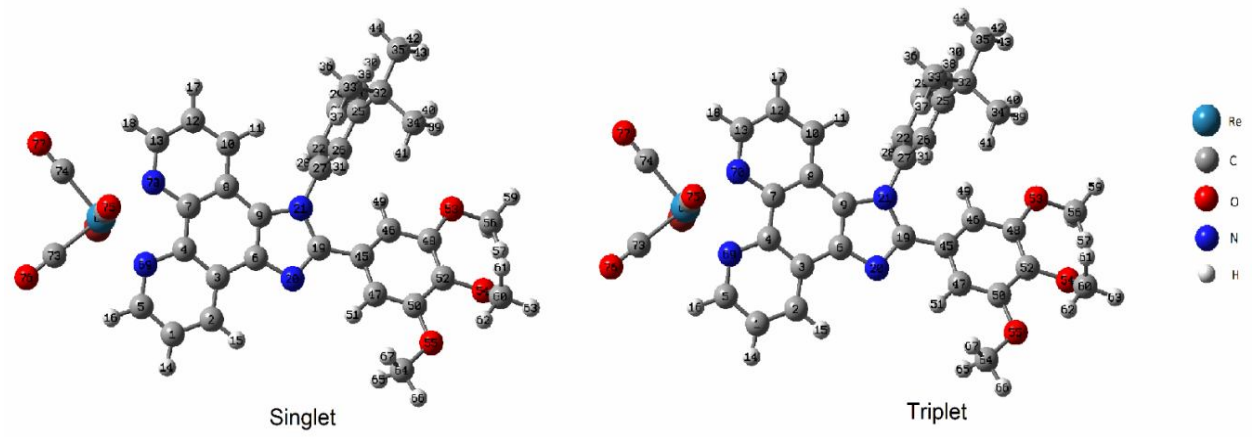

Fig. 2. Optimized structures of the singlet states (S_0, S_1, S_2, S_3, S_4) and triplet states (T_1, T_2, T_3 and T_4) of fac-[ReBr(CO)$_3$(L6)], complex 2.

Table 1. Dihedral Angles of the Singlet States (S_0, S_1, S_2, S_3, S_4) and Triplet States (T_1, T_2, T_3 and T_4) of fac-[ReBr(CO)$_3$(L4)], Complex 1

Dihedral[a]	Singlet	Triplet
D1	179.0530	168.9820
D2	-126.1653	-88.8634
D3	149.3176	138.1568

[a]D1, D2 and D3 are dihedral angles between O64, C61, Re57, C4 atoms, between O65, C62, Re57, C4 atoms and between O66, C63, Re57, C4 atoms, respectively.

Table 2. Dihedral Angles of the Singlet States (S_0, S_1, S_2, S_3, S_4) and Triplet States (T_1, T_2, T_3 and T_4) of fac-[$ReBr(CO)_3(L6)$], complex 2

Dihedral[a]	Singlet	Triplet
D1	-165.3243	172.8400
D2	-135.5600	-88.1202
D3	142.1838	123.8133

[a]D1, D2 and D3 are dihedral angle between O75, C72, Re68, C4 atoms, between O76, C73, Re68, C4 atoms and between O77, C74, Re68, C4 atoms, respectively.

Table 3. The TD-DFT Low-lying Singlet and Triplet States in the Gas Phase of fac-[Re $Br(CO)_3(L4)$], Complex 1

fac-[$ReBr(CO)_3(L4)$] Complex	State	Transition energy (ev)	Wavelength (nm)	Oscillator strength
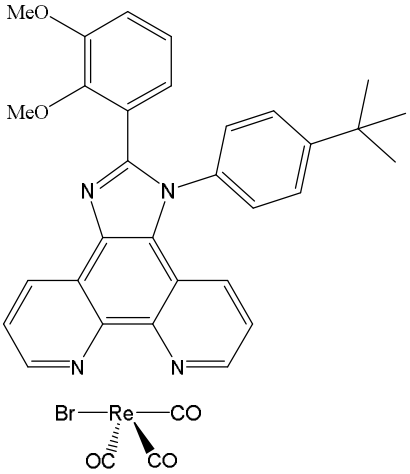	T_1	1.8674	663.94	
	S_1	2.6086	475.29	0.0013
	T_2	2.1877	566.74	
	S_2	2.7863	444.98	0.0426
	T_3	2.5294	490.18	
	S_3	3.0266	409.66	0.0212
	T_4	2.6416	469.35	
	S_4	3.0491	406.63	0.0220

than those in the gas phase. The oscillator strength of complex 1 is 0.0030 for $S_0 \rightarrow S_1$. This is more than that in the gas phase. The $S_0 \rightarrow S_3$ transition (f = 0.1091) is more strongly allowed than $S_0 \rightarrow S_1$.

In Table 6, the maximum absorption wavelengths and transition energy and oscillator strength for $S_0 \rightarrow S_1$ of complex 2 in the solution phase are 407.46, 3.0429 and 0.0385, respectively. The maximum luminescence wavelengths and transition energy for $T_1 \rightarrow S_0$ are 609.67 (nm) and 2.0336 (eV), respectively. As can be noted, the maximum wavelengths for S_1 and T_1 in the solution phase are shorter than those in the gas phase. The oscillator strength for $S_0 \rightarrow S_3$ (f = 0.0868) is greater than that for $S_0 \rightarrow S_1$ and probably is stronger than that for $S_0 \rightarrow S_1$.

The UV-Vis absorption spectra of singlet and luminescence spectra of triplet in the solution phase compared to the gas phase are presented in Fig. 7.

In the solution phase, the wavelengths for the absorption

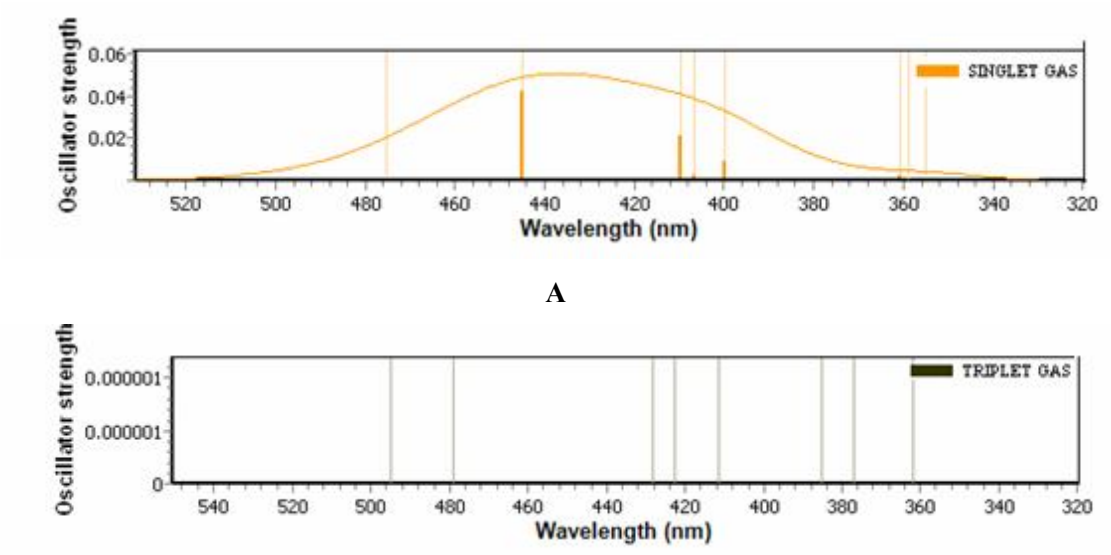

Fig. 3. A) The UV-Vis absorption spectra of the singlet states, and B) the UV-Vis luminescence spectra of the triplet states in the gas phase of fac-[$ReBr(CO)_3(L4)$], complex 1.

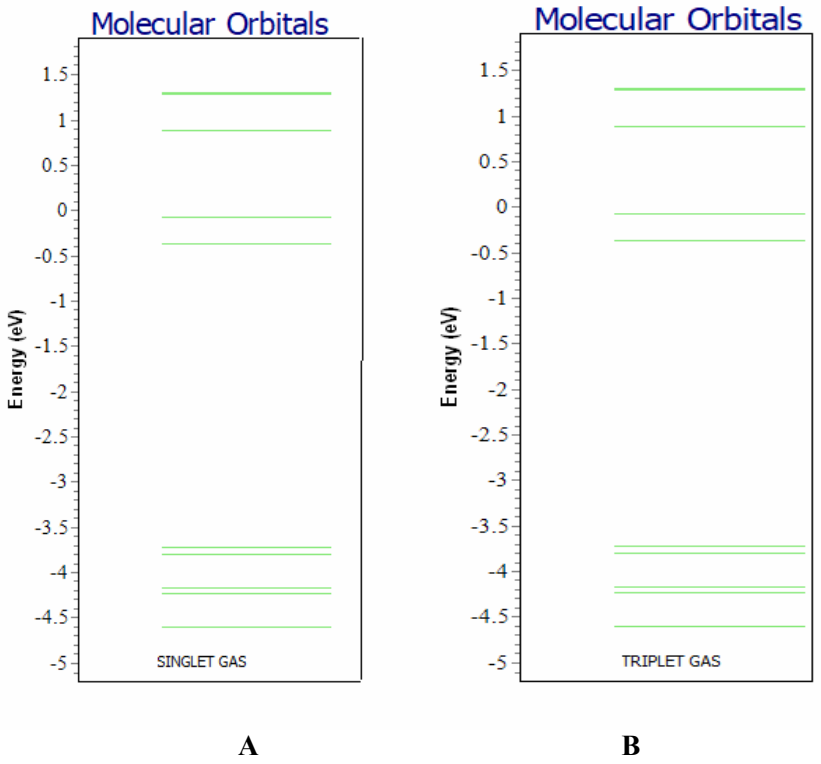

Fig. 4. The energy diagram of A) singlet states; B) triplet states in the gas phase of fac-[$ReBr(CO)_3(L4)$], complex 1.

Table 4. TD-DFT Low-lying Singlet and Triplet States in the Gas Phase of fac-[Re Br$(CO)_3$(L6)], Complex 2

fac-[ReBr(CO)3(L6)] Complex	State	Transition energy (eV)	Wavelength (nm)	Oscillator strength
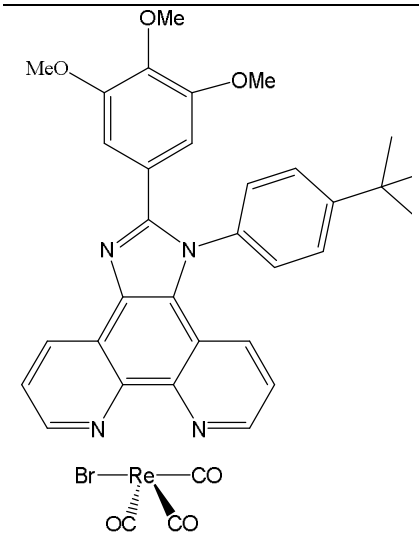	T_1	1.8556	668.17	
	S_1	2.5919	478.36	0.0012
	T_2	2.1726	570.68	
	S_2	2.7686	447.83	0.0459
	T_3	2.3781	521.37	
	S_3	3.0077	412.22	0.0231
	T_4	2.5539	485.47	
	S_4	3.0343	408.61	0.0014

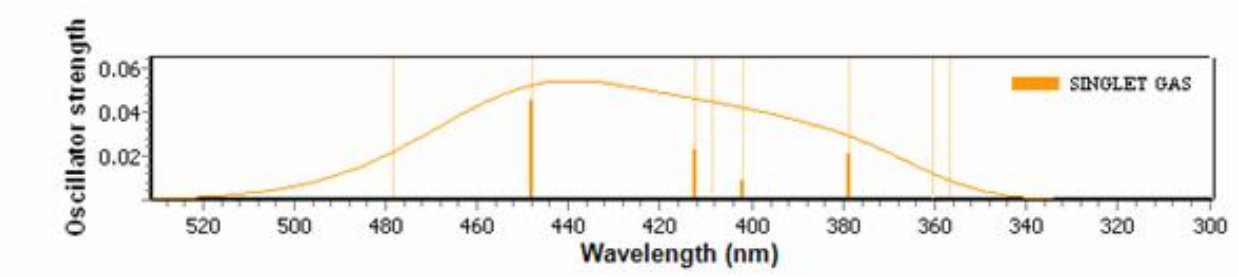

A

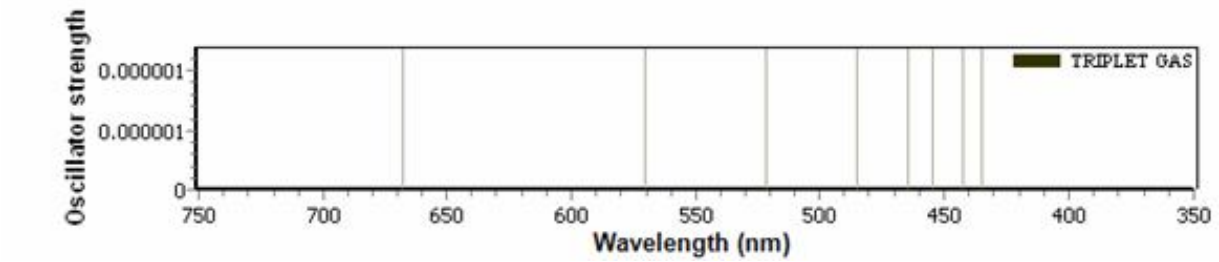

B

Fig. 5. A) The UV-Vis absorption spectra of the singlet states, and B) the UV-Vis luminescence spectra of the triplet states in the gas phase of fac-[ReBr$(CO)_3$(L6)], complex 2.

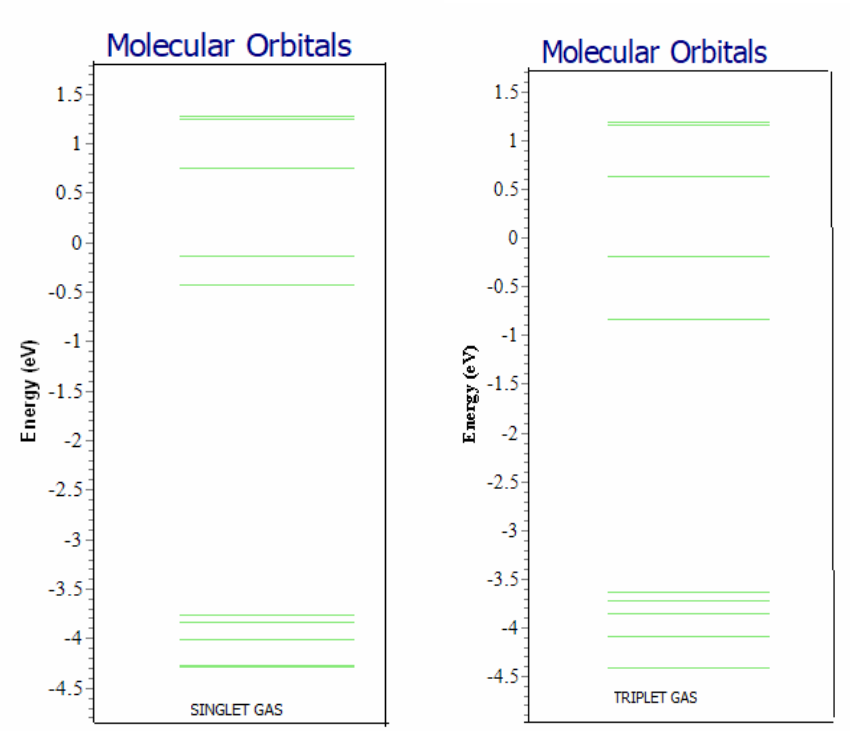

Fig. 6. The energy diagram of A) singlet states, and B) triplet states in the gas phase of fac-[$ReBr(CO)_3$ (L6)], complex 2.

Table 5. TD-DFT Low-lying Singlet and Triplet States in the Chloroform Phase of fac-[$ReBr(CO)_3$(L4)], Complex 1

State	Transition energy (eV)	Wavelength (nm)	Oscillator strength
T_1	2.0617	601.36	
S_1	3.0535	406.05	0.0030
T_2	2.3889	519.00	
S_2	3.1909	388.56	0.0049
T_3	2.5176	492.46	
S_3	3.2636	379.90	0.1091
T_4	2.7838	445.37	
S_4	3.3033	375.34	0.0014

Table 6. The TD-DFT Low-lying Singlet and Triplet States in the Chloroform Phase of fac-[$ReBr(CO)_3$(L6)], Complex 2

State	Transition energy (eV)	Wavelength (nm)	Oscillator Strength
T_1	2.0336	609.67	
S_1	3.0429	407.46	0.0028
T_2	2.2595	548.72	
S_2	3.1143	398.11	0.0483
T_3	2.4978	496.37	
S_3	3.2620	380.09	0.0868
T_4	2.6163	473.90	
S_4	3.2945	376.34	0.0053

spectra of the singlet excited state, and the wavelengths for the luminescence spectra of the triplet excited state are shorter than those of the gas phase and, therefore, its energies are more than those of the gas phase, and moreover, the oscillator strength for the solution phase is stronger than those of the gas phase.

SOC Calculations

Spin-orbit coupling (SOC) calculations of the electronic absorption spectra consistently point to large densities of low-lying spin-orbit states and wide singlet-triplet that their mixing makes vain the isolation/interpretation of pure singlet and triplet electronic states [32-35]. A linear combination of scalar singlet-singlet and singlet-triplet excitations was used in each SOC transition.

The absorption spectrum *via* transition electronic dipole moment and SOC corrected absorption spectrum *via* transition electronic dipole moment of the complexes 1 and 2 are demonstrated in Fig. 8 in both phases. The calculated wavelengths are shorter than those obtained before SOC calculations for complexes 1 and 2 in the gas and the solution phases. Also, the wavelength of the solution phase before and after SOC is shorter than those of the gas phase. In general, the wavelength range is increased, and λ_{max} splits and is shifted, especially in complex 2 after SOC. The λ_{max} values of the absorption before and after SOC in the gas phase are 444 nm (0.194 intensity) and 440 nm (0.125 intensity), respectively, (Fig. 8A), and in the solution phase are 397 nm (0.122 intensity) and 394 nm (0.102 intensity), respectively, (Fig. 8B) for the complex 1. For the complex 2, they are 461 nm (0.152 intensity) and 458 nm (0.087 intensity), respectively, in the gas phase (Fig. 8C), and are 393 nm (0.187 intensity) and 391 nm (0.171 intensity), respectively, in the solution (Fig. 8D) (see Table 7). The evaluated diagrams before and after SOC, drawn by Multiwfn 3.6 software, [50] are shown as Figs. 1S and 2S.

Table 7 presents the outcomes of metal to ligand charge transfer (MLCT) in the gas phase, chloroform phase, and experiment for the singlet and triplet states of complexes, the triplet state of free ligands, and SOC in gas and solution phases of L4 and L6. Table 7 illustrates the experimental results in the solution phase at a level of 1×10^{-5} M. Very low concentrations have been utilized for the chloroform solvent in experimental work. Also, for the free ligands, the outcomes of the triplet state are close to the outcomes of the singlet complexes in a solution state, both in computational and experimental methods. The transition states for SOC

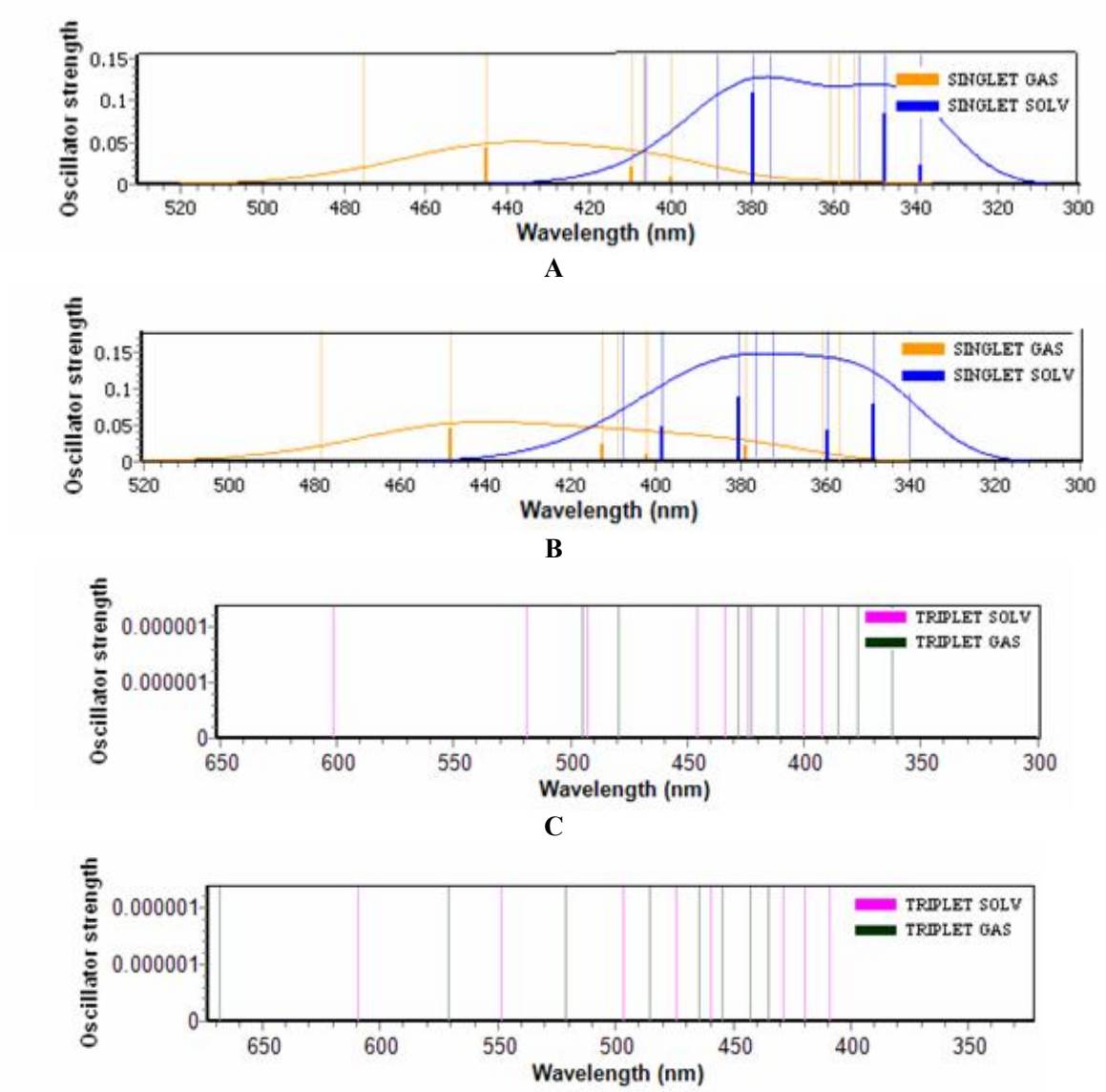

Fig. 7. A, B) The UV-Vis absorption spectra of the singlet states of complex 1 and 2, respectively; C, D) the UV-Vis luminescence spectra of the triplet states of complex 1 and 2, respectively, in solution and gas phases.

show blue shifts in complexes 1 and 2 in the solution phase in comparison to the experimental data.

NBO Calculations

NBO analysis [51,52] demonstrated the role of intermolecular interactions in the complexes. It highlights the role of intermolecular orbital interactions in the complex, mainly charge transfer. For this purpose, it is necessary to consider all likely interactions between filled donor and empty acceptor NBOs and estimate their energetic importance. The stabilization energy, E(2), for each donor NBO (i) and acceptor NBO (j), related to the electron delocalization between the donor and the acceptor was estimated as:

$$E(2) = -q_i \frac{F_{(ij)}^2}{\varepsilon_i - \varepsilon_j}$$

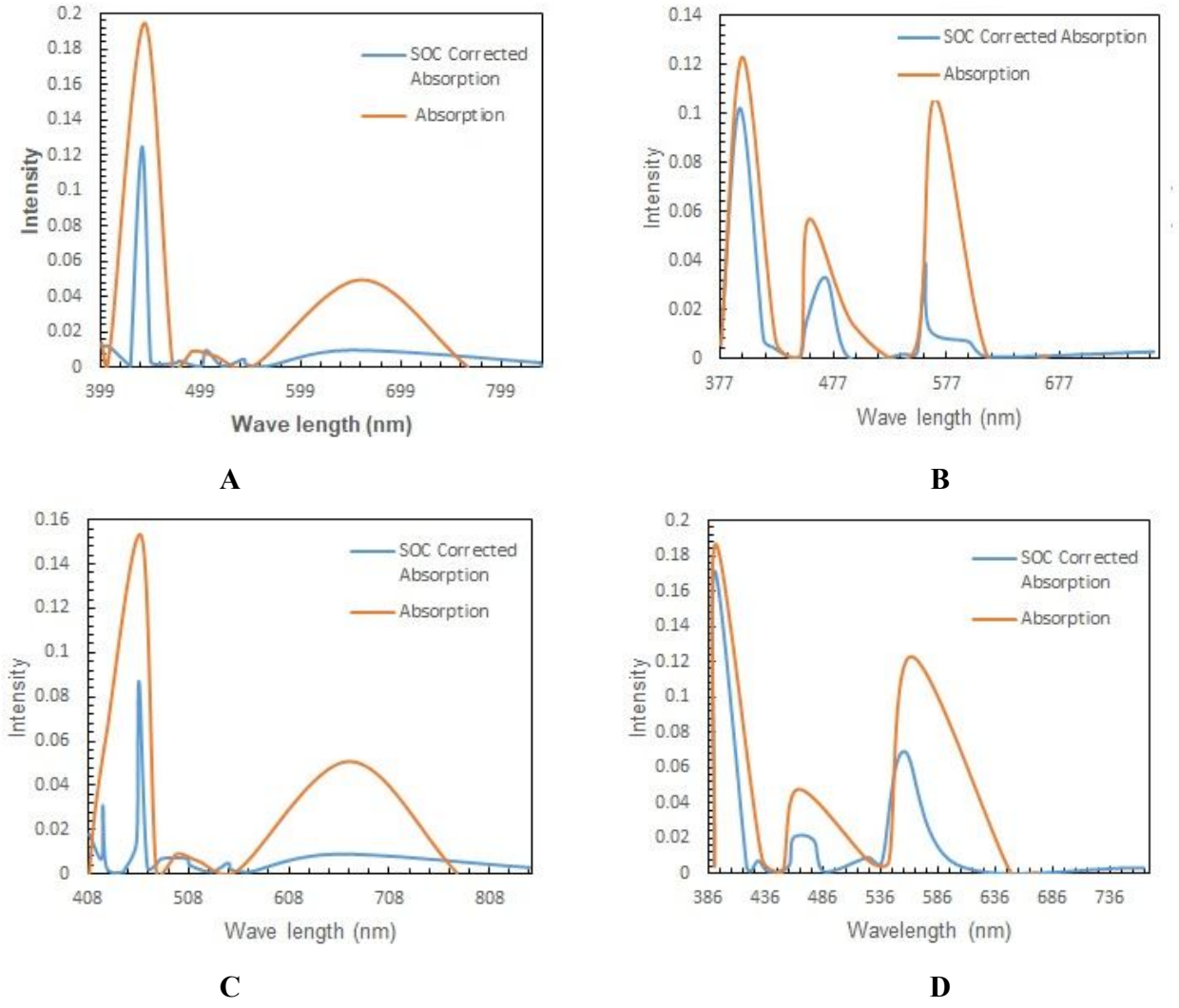

Fig. 8. The absorption spectrum and SOC corrected absorption spectrum of complexes 1 and 2 in the gas and the solution phases, (A and B) and (C and D)), respectively.

where q_i refers to the donor orbital occupancy, ε_i and ε_j represent diagonal elements (orbital energies), respectively, and $F_{(IJ)}$ represent the off-diagonal NBO Fock matrix element. The stabilization energy, E(2), offers a quantitative standard for the strength relating to the interaction between an electron donor and the receptor. A greater E(2) means a stronger interaction between the electron donor orbital i and the acceptor orbital j. Also, the orbital i shows more tendency to give an electron to the orbital j.

Table 8 shows the data analysis resulting from NBO calculations for the single and triple modes of two complexes in solution phase. Table 8 presents only significant amounts of energy greater than 20 (kcal mol^{-1}) for states in which rhenium metal was utilized as a donor or acceptor of electrons. The summation of transition energy in the NBO calculations was measured for transferring

Table 7. S_1 and T_1 States of 1 and 2 Complexes for Gas and Solution Phases with Chloroform as Solvent and Experimental Data

Physical State	Transition State	fac-[ReBr(CO)$_3$(L4)]	fac-[Re Br(CO)$_3$(L6)]
Gas	S_1	445	448
Solution	S_1	380	380
experimental data[a]	S_1	418	426
Gas	T_1	664	668
Solution	T_1	601	610
experimental data[a]	T_1	580	580
solution free ligand	T_1	499	506
experimental free ligand[a]	T_1	399	419
Gas	SOC	440	458
Solution	SOC	397	391

[a]The reported experimental data refer to (Ref. [45]).

electrons from the rhenium metal as a donor and the ligand as the acceptor, as well as the other states of the ligand as the donor and the rhenium metal as the acceptor. This value represents that the summation of the transition energy of rhenium metal to the ligand is greater than the summation of the transition energy from the ligand to rhenium metal. For example, in the NBO calculations of complex 1, the summation of Re → L4 transition energy is 563.75 (kcal mol^{-1}) and the summation of L4 → Re transition energy is 465.94 (kcal mol^{-1}).

Based on the data presented in Table 8, the antibonding orbitals corresponding to the acceptor are able to interact with the lone pairs of N(58), N(59) and Br(60) of singlet and triplet states of complex 1 and N(69), N(70) and Br(71) of the singlet and triplet states of complex 2 as the donor orbital. In the singlet state of complex 1, the greatest E(2) values are observed in the $n_{(x)N58} \rightarrow n^*_{(x)Re57}$ and $n_{(X)Br60} \rightarrow n^*_{(Z)Re57}$ interactions. For the triplet of this complex, the maximum amounts of E(2) are found in the $n_{(X)N58} \rightarrow n^*_{(y)Re57}$ and $n_{(X)Br60} \rightarrow n^*_{(Z)Re57}$ interactions. For the singlet state of complex 2, the greatest E(2) values appear in the $n_{(X)N69} \rightarrow n^*_{(x)Re68}$ and $n_{(X)Br71} \rightarrow n^*_{(Z)Re68}$ interactions. For triplet of this complex, the maximum E(2) values appear in the $n_{(X)N69} \rightarrow n^*_{(x)Re68}$ and $n_{(X)Br71} \rightarrow n^*_{(Z)Re68}$ interactions. The greatest partial electron transfer (Q) in the singlet and triplet states for two complexes is associated to the electron transition between N, Br and Re, that led to a high luminescence. In complex 2, Q is more than that in complex 1.

CONCLUSIONS

In this work, complexes 1 and 2 were optimized under Cs symmetry group. In the triplet excited states T_1, T_2, T_3 and T_4 and in the singlet electronic ground state, the lowest S_1, S_2, S_3 and S_4 singlet excited states were calculated vertical excitations at the ground state geometry in gas phase and in chloroform solvent. The results of the absorption wavelengths, transition energy, and oscillator strength for the triplet states in the solution phase are closer to the experimental data. The spin-orbit coupling (SOC) calculations show sufficient intensity and short wavelength in the UV-Vis absorption after SOC correction. The UV-Vis absorption spectra for the SOC transition show blue shifts in complexes 1 and 2 in gas and solution phases. The summation of transition energy of rhenium metal to the

Table 8. Some Significant Second-order Interaction Energies (E(2), kcal mol^{-1}) and Partial Electron Transfer (q) between Donor and Acceptor Orbitals in the Singlet and Triplet States of Complex 1 and Complex 2 in Solution Phase Calculated at the B3LYP/lanl2mb Level of Theory

Complex	Donor (i)	Acceptor (j)	E(2) (kcal mol^{-1})	Q (me)
Singlet L4	$n_{(x)N58}$	$n^*_{(x)Re57}$	91.52	0.1044
	$n_{(x)N58}$	$n^*_{(y)Re57}$	37.68	0.1038
	$n_{(x)N58}$	$\delta^*_{Re57-C63}$	43.46	0.0942
	$n_{(x)N59}$	$n^*_{(x)Re57}$	60.93	0.1038
	$n_{(x)N59}$	$n^*_{(y)Re57}$	67.26	0.1048
	$n_{(x)N59}$	$\delta^*_{Re57-C62}$	42.97	0.0959
	$n_{(x)Re57}$	$\pi^*_{C62-O65}$	37.57	0.0970
	$n_{(x)Re57}$	$\pi^*_{C63-O66}$	36.35	0.0963
	$n_{(y)Re57}$	$\pi^*_{C61-O64}$	50.65	0.0955
	$n_{(z)Re57}$	$\delta^*_{C61-O64}$	44.25	0.0921
	$n_{(x)Br60}$	$n^*_{(z)Re57}$	88.55	0.1067
	$n_{(x)Br60}$	$\delta^*_{Re57-C61}$	24.26	0.0967
Triplet L4	$n_{(x)N58}$	$n^*_{(x)Re57}$	49.52	0.1029
	$n_{(x)N58}$	$n^*_{(y)Re57}$	88.49	0.1041
	$n_{(x)N58}$	$\delta^*_{Re57-C63}$	48.80	0.0942
	$n_{(x)N59}$	$n^*_{(x)Re57}$	58.47	0.1042
	$n_{(x)N59}$	$n^*_{(y)Re57}$	68.19	0.1049
	$n_{(x)N59}$	$\delta^*_{Re57-C62}$	42.89	0.0942
	$n_{(x)Re57}$	$\pi^*_{C62-O65}$	39.25	0.0964
	$n_{(x)Re57}$	$\pi^*_{C63-O66}$	33.79	0.0968
	$n_{(y)Re57}$	$\pi^*_{C61-O64}$	46.86	0.0946
	$n_{(z)Re57}$	$\delta^*_{C61-O64}$	43.51	0.0927
	$n^*_{(y)Re57}$	$\delta^*_{C61-O64}$	52.05	0.0200
	$n_{(x)Br60}$	$n^*_{(z)Re57}$	85.95	0.1059
	$n_{(x)Br60}$	$\delta^*_{Re57-C61}$	22.63	0.0958

Table 8. Continued

Singlet L6	$n_{(x)N69}$	$n^*_{(x)Re68}$	90.68	0.1045
	$n_{(x)N69}$	$n^*_{(y)Re68}$	38.3	0.1061
	$n_{(x)N69}$	$\delta^*_{Re68-C74}$	43.46	0.0942
	$n_{(x)N70}$	$n^*_{(x)Re68}$	61.79	0.1039
	$n_{(x)N70}$	$n^*_{(y)Re68}$	66.37	0.1047
	$n_{(x)N70}$	$\delta^*_{Re68-C73}$	42.99	0.0944
	$n_{(x)Re68}$	$\pi^*_{C73-O76}$	37.26	0.0962
	$n_{(x)Re68}$	$\pi^*_{C74-O77}$	36.4	0.0964
	$n_{(y)Re68}$	$\pi^*_{C72-O75}$	50.72	0.0956
	$n_{(z)Re68}$	$\delta^*_{C72-O75}$	44.25	0.0921
	$n^*_{(x)Re68}$	$\delta^*_{C72-O75}$	50.72	0.0373
	$n^*_{(y)Re68}$	$\delta^*_{C72-O75}$	41.4	0.0347
	$n_{(X)Br71}$	$n^*_{(z)Re68}$	88.54	0.1067
	$n_{(X)Br71}$	$\delta^*_{Re68-C72}$	24.28	0.0968
Triplet L6	$n_{(x)N69}$	$n^*_{(y)Re68}$	115.39	0.1047
	$n_{(x)N69}$	$\delta^*_{Re68-C74}$	48.81	0.0942
	$n_{(x)N70}$	$n^*_{(x)Re68}$	87.01	0.1037
	$n_{(x)N70}$	$n^*_{(y)Re68}$	39.71	0.1047
	$n_{(x)N70}$	$\delta^*_{Re68-C73}$	42.87	0.0942
	$n_{(x)Re68}$	$\pi^*_{C73-O76}$	39.31	0.0966
	$n_{(x)Re68}$	$\pi^*_{C74-O77}$	33.7	0.0966
	$n_{(y)Re68}$	$\pi^*_{C72-O75}$	47.13	0.0951
	$n_{(y)Re68}$	$\delta^*_{C73-O76}$	24.76	0.0945
	$n_{(z)Re68}$	$\delta^*_{C72-O75}$	43.68	0.0930
	$n^*_{(y)Re68}$	$\delta^*_{C72-O75}$	50.36	0.0211
	$n_{(X)Br71}$	$n^*_{(z)Re68}$	85.91	0.1059
	$n_{(X)Br71}$	$\delta^*_{Re68-C73}$	22.64	0.0959

ligand is greater than the summation of transition energy from the ligand to rhenium metal. So, rhenium metal shows more tendency to give an electron to ligand. The maximum E(2) values appear between Re and N, Br atoms. In complex 2, Q is more than that in complex 1. Thus this property can be used in cell imaging agents, chemosensors and OLED applications.

ACKNOWLEDGMENTS

Authors would like to thank the Salahaddin University-erbil for its support. Gaussian 09 was used as the calculation software in this study, with CI reference number: 57295 and Invoice number: ACI-564467081250. The Chemissian, version 4.23, software was free and used online from the website, www.chemissian.com

REFERENCES

[1] Stufkens, D. J.; Vlˇcek Jr, A., Ligand-dependent excited state behaviour of Re(I) and Ru(II) carbonyl-diimine complexes. *Coord. Chem. Rev.* **1998**, *177*, 127-179, DOI: 10.1016/S0010-8545(98)00132-5.

[2] Vlˇcek Jr, A., Photophysics and photochemistry of organometallic rhenium diimine complexes: From excitation to photochemistry. *Top. Chem.* **2010**, *29*, 73-114, DOI: 10.1007/3418_2009_4.

[3] Kumar, A.; Sun, S. -S.; Lees, A. J., Photophysics and photochemistry of organometallic rhenium diimine complexes. *Top. Organomet. Chem.* **2010**, *29*, 1-35, DOI: 10.1007/3418_2009_2.

[4] Hawecker, J.; Lehn, J. -M.; Ziessel, R., Efficient photochemical reduction of CO_2 to CO by visible light irradiation of systems containing $Re(bipy)(CO)_{3X}$ or Ru(bipy)32+–Co2+ combinations as homogeneous catalysts. *J. Chem. Soc., Chem. Commun.* **1983**, *9*, 536-538, DOI: 10.1039/C39830000536.

[5] Takeda, H.; Koike, K.; Inoue, H.; Ishitani, O., Development of an efficient photocatalytic system for CO2 reduction using rhenium(I) complexes based on mechanistic studies. *J. Am. Chem. Soc.* **2008**, *130*, 2023-2031, DOI: 10.1021/ja077752e.

[6] Morimoto, T.; Nakajima, T.; Sawa, S.; Nakanishi, R.; Imori, D.; Ishitani, O., CO_2 Capture by a rhenium(I) complex with the aid of triethanolamine. *J. Am. Chem. Soc.* **2013**, *135*, 16825-16828, DOI: 10.1021/ja409271s.

[7] Kam. K.; Lo, W., Exploitation of luminescent organometallic rhenium(I) and iridium(III) complexes in biological studies. *Top Organomet. Chem.* **2010**, *29*, 115-158, DOI: 10.1007/3418_2009_3.

[8] Lo, K. K. -W.; Sze, K. -S.; Tsang, K. H. -K.; Zhu, N., Luminescent tricarbonyl rhenium(I) dipyridoquin-oxaline iodine complexes as sensitive probes for indole-binding proteins. *Org. Met.* **2007**, *26*, 3440-3447, DOI: 10.1021/om0700617.

[9] Sajoto, T.; Djurovich, P. I.; Tamayo, A. B.; Oxgaard, J.; Goddard, W. A.; Thompson, M. E., Temperature dependence of blue phosphorescent cyclometalated Ir(III) complexes. *J. Am. Chem. Soc.* **2009**, *131*, 9813-9822, DOI: 10.1021/ja903317w.

[10] Balakrishna, M. S.; Suresh, D.; Rai, A.; Mague, J. T.; Panda, D., Dinuclear copper(I) complexes containing cyclodiphosphazane derivatives and pyridyl ligands: synthesis, structural studies, and antiproliferative activity toward human cervical and breast cancer cells. *Inorg. Chem.* **2010**, *49*, 8790-8801, DOI: 10.1021/ic100944d.

[11] Peacock, A. F. A.; Batey, H. D.; Raendler, C.; Whitwood, A. C.; Perutz, R. N.; Duhme-Klair, A. -K., A metal-based lumophore tailored to sense biologically relevant oxometalates. *Angew. Chem. Int. Ed.* **2005**, *44*, 1712-1714, DOI: 10.1002/anie.200462306.

[12] Lewis, J. D.; Moore, J. N., Cation sensors containing a $(bpy)Re(CO)_3$ group linked to an azacrown ether *via* an alkenyl or alkynyl spacer: synthesis, characterisation, and complexation with metal cations in solution. *Dalt. Trans.* **2004**, *9*, 1376-1385, DOI: 10.1039/b401092b.

[13] Blanco-Rodriguez, A. M.; Kvapilova, H.; Sykora, J.; Towrie, M.; Nervi, C.; Volpi, G.; Zalis, S.; Vlˇcek Jr, A., Photophysics of singlet and triplet intraligand excited statesin $[ReCl(CO)_3$(1-(2-pyridyl)-imidazo [1,5-α]pyridine)] complexes. *J. Am. Chem. Soc.* **2014**, *136*, 5963-5973, DOI: 10.1021/ja413098m.

[14] Patrocinio, A. O. T.; Iha, N. Y. M., Photoswitches and

and luminescent rigidity sensors based on fac-$[Re(CO)_3(Me_4phen)(L)]^+$. *Iha, Inorg. Chem.* **2008**, *47*, 10851-10857, DOI: 10.1021/ic800504a.

[15] Polo, A. S.; Itokazu, M. K.; Frin, K. M.; de Toledo Patrocinio, A. O.; Murakami Iha, N. Y., Light driven *trans*-to-*cis* isomerization of stilbene-like ligands in fac-$[Re(CO)_3(NN)(trans\text{-}L)]^+$ and luminescence of their photoproducts. *Coord. Chem. Rev.* **2006**, *250*, 1669-1680, DOI: 10.1016/j.ccr.2005.12.015.

[16] Beyeler, A.; Belser, P.; Cola, L. D., Rhenium complexes with a photochemically variable anthracene subunit: A molecular switch. *Angew. Chem. Int. Ed. Engl.* **1997**, *36*, 2779-2781, DOI: org/10.1002/anie.199727791.

[17] Cleland, D. M.; Irwin, G.; Wagner, P.; Officer, D. L.; Gordon, K. C., Linker conjugation effects in rhenium(I) bifunctional hole transport/emitter molecules. *Chem. Eur. J.* **2009**, *15*, 3682-3690, DOI: 10.1002/chem.200802373.

[18] Ellingson, R. J.; Asbury, J. B.; Ferrere, S.; Ghosh, H. N.; Sprague, J. R.; Lian, T.; Nozik, A. J., Dynamics of electron injection in nanocrystalline titanium dioxide films sensitized with [Ru(4,4‘-dicarboxy-2,2‘-bipyridine)$_2$(NCS)$_2$] by Infrared transient absorption. *J. Phys. Chem. B.* **1998**, *102*, 6455-6458, DOI: 10.1021/jp982310y.

[19] Blanco-Rodríguez, A. M.; Busby, M.; Ronayne, K.; Towrie, M.; Gradinaru, C.; Sudhamsu, J.; Sy´kora, J.; Hof, M.; Za´liš˘, S.; Di Bilio, A. J.; Crane, B. R.; Gray, H. B.; Vlc˘ek, Jr, A., Relaxation dynamics of pseudomonas aeruginosa $ReI(CO)_3$ (α-diimine)$(HisX)^+$ (X = 83, 107, 109, 124, 126)Cu II azurins, *J. Am. Chem. Soc.* **2009**, *131*, 11788-11800, DOI: 10.1021/ja902744s.

[20] Blanco-Rodríguez, A. M.; Busby, M.; Gradinaru , C.; Crane, B. R.; Di Bilio, A. J.; Matousek, P.; Towrie, M.; Leigh, B. S.; Richards, J. H.; Vlc˘ek, Jr, A.; Gray, H. B., Excited-state dynamics of structurally characterized $[ReI(CO)_3(phen)(HisX)]^+$ (X = 83, 109) pseudomonas aeruginosa azurins in aqueous solution. *J. Am. Chem. Soc.* **2006**, *128*, 4365-4370, DOI: 10.1021/ja057451.

[21] Sazanovich, I. V.; Alamiry, M. A. H.; Best, J.; Bennett, R. D.; Bouganov, O. V.; Davies, E. S.; Grivin, V. P.; Meijer, A. J. H. M.; Plyusnin, V. F.; Ronayne, K. L.; Shelton, A. H.; Tikhomirov, S. A.; Towrie, M.; Weinstein, J. A.; Excited state dynamics of a PtII diimine complex bearing a naphthalene-diimide electron acceptor. *Inorg. Chem.* **2008**, *47*, 10432-10445, DOI: 10.1021/ic801022h.

[22] Blanco-Rodríguez, A. M.; Towrie, M.; Collin, J. -P.; Záliš, S.; Vl˘cek Jr, A., Excited-state relaxation dynamics of Re(I) tricarbonyl complexes with macrocyclic phenanthroline ligands studied by time-resolved IR spectroscopy. *Dalt. Trans.* **2009**, *20*, 3941-3949, DOI: 10.1039/b820748h.

[23] Shih, C.; Museth, A. K.; Abrahamsson, M.; Blanco-Rodríguez, A. M.; Di Bilio, A. J.; Sudhamsu, J.; Crane, B. R.; Ronayne, K. L.; Towrie, M.; Vlc˘ek Jr, A.; Richards, J. H.; Winkler, J. R.; Gray, H. B., Tryptophan-accelerated electron flow through proteins. *Science.* **2008**, *320*, 1760-1762, DOI: 10.1126/science.1158241.

[24] Blanco-Rodríguez, A. M.; Di Bilio, A. J.; Shih, C.; Museth, A. K.; Clark, I. P.; Towrie, M.; Cannizzo, A.; Sudhamsu, J.; Crane, B. R.; Sýkora, J.; Winkler, J. R.; Gray, H. B.; Záliš, S.; Vl˘cek Jr, A., Phototriggering electron flow through Re(I)-modified pseudomonas aeruginosa azurins. *Chem. Eur. J.* **2011**, *17*, 5350-5361, DOI: 10.1002/chem.201002162.

[25] Heitz, M. -C.; Ribbing, C.; Daniel, C., Spin-orbit induced radiationless transitions in organometallics: Quantum simulation of the intersystem crossing processes in the photodissociation of $HCo(CO)_4$. *J. Chem. Phys.* **1997**, *106*, 1421-1428, DOI: 10.1063/1.473291.

[26] Taylor, P. N.; Anderson, H. L., Cooperative self-assembly of double-strand conjugated porphyrin ladders. *J. Am. Chem. Soc.* **1999**, *121*, 11538-11545, DOI: 10.1021/ja992821d.

[27] Bruand-Cote, I.; Daniel, C., Photodissociation and electronic spectroscopy of $[Re(H)(CO)_3(H\text{-}dab)]$ (H-dab = 1,4-diaza-1,3-butadiene): quantum wavepacket dynamics based on ab initio potentials. *Chem. Eur. J.* **2002**, *8*, 1361-1371, DOI: 10.1002/1521-3765.

[28] Li, X.; Zhang, D.; Li, W.; Chu, B.; Han, L.; Zhu, J.; Su, Z.; Bi, D.; Wang, D.; Yang, D.; Chen, Y. Very high-efficiency organic light-emitting diodes based on

cyclometallated rhenium(I) complex. *Appl. Phys. Lett.* **2008**, *92*, 083302-1-3, DOI: doi:10.1063/1.2888767.

[29] Minaev, B.; Baryshnikov, G.; Agren, H., Principles of phosphorescent organic light emitting devices. *Phys. Chem. Chem. Phys.* **2014**, *16*, 1719-1758, DOI: 10.1039/c3cp53806k.

[30] Gama, P. E.; Corrêa, R. J.; Garden, S. J., Synthesis, characterization and photophysical study of ethynyl pyrene derivatives as promising materials for organic optoelectronics. *J. Lumines.* **2015**, *61*, 37-46, DOI: 10.1016/j.jlumin.2014.12.036.

[31] Barani, E.; Izadyar, M.; Housaindokht, M.R., QM/MM study on the mechanism of aminophenol oxidation by functionalized β-cyclodextrin as oxidase nanomimic. *Phys. Chem. Res.* **2016**, *4*, 519-530, DOI: 10.22036/pcr.2016.15366.

[32] Ahmadi, R.; Ebrahimikia, M.; Calculation of thermodynamic parameters of [2.4.6] three nitro toluene (TNT) with nanostructures of fullerene and boron nitride nano-cages over different temperatures, using density functional theory. *Phys. Chem. Res.* **2017**, *5*, 617-627, DOI: 10.22036/pcr.70859.1337.

[33] Kancheva, P. B.; Delchev, V. B., Comparative study of the gas-phase cyclodimer formations of uracil and 6-azauracil in excited state and through conical intersections S0/S1. *Acta Chim. Slov.* **2018**, *65*, 521-530, DOI: 10.17344/acsi.2017.4040.

[34] Li, X.; Minaev, B.; Ågren, H.; Tian, H., Density functional theory study of photophysical properties of iridium(III) Complexes with phenylisoquinoline and phenylpyridine ligands. *J. Phys. Chem. C* **2011**, *115*, 20724-20731, DOI: 10.1021/jp206279g.

[35] Jayabharathi, J.; Thanikachalam, V.; Jayamoorthy, K., Photophysical studies of some heterocyclic chromophores as potential NLO materials. *J. Spectrochim. Acta A* **2012**, *89*, 301-307, DOI: 10.1016/j.saa.2011.12.031.

[36] Cannizzo, A.; Blanco- Rodríguez, A. M.; El Nahhas, A.; Sebera, J.; Zális, S.; Vl˘cek Jr, A., Chergui, M., Femtosecond fluorescence and intersystem crossing in rhenium(I) carbonyl-bipyridine complexes. *J. Am. Chem. Soc.* **2008**, *130*, 8967-8974, DOI: 10.1021/ja710763w.

[37] Yanover, D.; Kaftory, M., Structural comparisons between methylated and unmethylated nitrophenyl lophines. *Acta Crystallorg. C* **2009**, *65*, o365-o370, DOI: 10.1107/S0108270109022203.

[38] Boyatzis, S.; Nikokavouras, J., Chemiluminescence of lophines in micellar media: irradiation-induced regeneration of *p*-dimethylaminolophine during the light reaction. *J. Photoch. Photobio. A* **1988**, *44*, 335-347, DOI: 10.1016/1010-6030(88)80104-7.

[39] Kishikawa, N.; Ohyama, K.; Saiki, A.; Matsuo, A.; Ali, M. F. B.; Wada, M.; Nakashima, K.; Kuroda, N., A novel lophine-based fluorescence probe and its binding to human serum albumin. *Anal. Chim. Acta.* **2013**, *780*, 1-6, DOI: 10.1016/j.aca.2013.04.003.

[40] Yagi, K.; Soong, C.F.; Irie, M., Synthesis of fluorescent diarylethenes having a 2,4,5-triphenylimidazole chromophore. *J. Org. Chem.* **2001**, *66*, 5419-5423. DOI: 10.1021/jo010267w.

[41] Feng, K.; Hsu, F. -L.; Van DerVeer, D.; Bota, K.; Bu, X.R., Tuning fluorescence properties of imidazole derivatives with thiophene and thiazole. *J. Photoch. Photobio. A* **2004**, *165*, 223-228, DOI: 10.1016/j.jphotochem.2004.03.021.

[42] Nakashima, K.; Yamasaki, H.; Kuroda, N.; Akiyama, S., Evaluation of lophine derivatives as chemiluminogens by a flow-injection method. *Anal. Chem. Acta.* **1995**, *303*, 103-107, DOI: 10.1016/0003-2670(94)00360-X.

[43] Cardinaels, T.; Ramaekers, J.; Nockemann, P.; Driesen, K.; Van Hecke, K.; Van Meervelt, L.; Lei, S.; De Feyter, S.; Guillon, D.; Donnio, B.; Binnemans, K., Imidazo[4,5-f]-1,10-phenanthrolines: versatile ligands for the design of metallomesogens. *Chem. Mater.* **2008**, *20*, 1278-1291, DOI: 10.1021/cm070637i.

[44] Liu, Y.; Tu, D.; Zhu, H.; Chen, X., Lanthanide-doped luminescent nano-probes: controlled synthesis, optical spectroscopy, and bioapplications. *Chem. Soc. Rev.* **2013**, *42*, 6924-6958, DOI: 10.1039/C3CS60060B.

[45] Bonello, R. O.; Pitak, M. B.; Coles, S. J.; Hallet, A. J.; Fallis, I. A.; Pope, S. J.A., Synthesis and characterisation of phosphorescent rhenium(I) complexes of hydroxy-and methoxy-substituted imidazo [4,5-f]-1,10-phenanthroline ligands. *J.*

Organomet Chem. **2017**, *841*, 39-47, DOI: org/10.1016/j.jorganchem.2017.04.021.

[46] Frisch, M. J.; Trucks, G. W.; Schlegel, H. B.; Scuseria, G. E.; Robb, M. A.; Cheeseman, J.R.; Scalmani, G.; Barone, V.; Mennucci, B.; Petersson, G. A.; Nakatsuji, H.; Caricato, M.; Li, X.; Hratchian, H.P.; Izmaylov, A. F.; Bloino, J.; Zheng, G.; Sonnenberg, J.L.; Hada, M.; Ehara, M.; Toyota, K.; Fukuda, R.; Hasegawa, J.; Ishida, M.; Nakajima, T.; Honda, Y.; Kitao, O.; Nakai, H.; Vreven, T.; Montgomery, J. A.; Peralta, J. E.; Ogliaro, F.; Bearpark, M.; Heyd, J. J.; Brothers, E.; Kudin, K. N.; Staroverov, V. N.; Kobayashi, R.; Normand, J.; Raghavachari, K.; Rendell, A.; Burant, J. C.; Iyengar, S. S.; Tomasi, J.; Cossi, M.; Rega, N.; Millam, J. M.; Klene, M.; Knox, J. E.; Cross, J. B.; Bakken, V.; Adamo, C.; aramillo, J.; Gomperts, R.; Stratmann, R. E.; Yazyev, O.; Austin, A. J.; Cammi, R.; Pomelli, C.; Ochterski, J. W.; Martin, R. L.; Morokuma, K.; Zakrzewski, V. G.; Voth, G. A.; Salvador, P.; Dannenberg, J. J.; Dapprich, S.; Daniels, A. D.; Farkas, J. B.; Foresman, J. V.; Ortiz, J.; Cioslowski, D. J., Fox: Wallingford CT, 2016. Gaussian 09, Revision A.02.

[47] Skripnikov, L., Chemissian, version 4.23, 2014, www.chemissian.com.

[48] Neese, F., The ORCA program system. Wiley Interdisciplinary Reviews: *Comp. Mol. Sci.* **2012**, *2*, 73-78, DOI:10.1002/wcms.81.

[49] Neese, F., Software update: The ORCA program system, version 4.0. Wiley Interdisciplinary Reviews: *Comp. Mol. Sci.* **2018**, *8*, e1327, DOI: 10.1002/ wcms.1327.

[50] Lu, T., Multiwfn, version 3.6, 2019, http://sobereva.com/multiwfn.

[51] Reed, A. E.; Curtiss, L. A.; Weinhold, F., Intermolecular interactions from a natural bond orbital, donor-acceptor viewpoint. *Chem. Rev.* **1988**, *88*, 899-926, DOI: 10.1021/cr00088a005.

[52] Yang, C.; Wang, H., *Ab initio* and DFT theory studies of interaction of thymine with formaldehyde. *Struct. Chem.* **2008**, *19*, 843-847, DOI: 10.1007/s11224-008-9374-z.